Published in final edited form as:
Nat Neurosci. 2012 June ; 15(6): 836–844. doi:10.1038/nn.3103.

Preso1 dynamically regulates group I metabotropic glutamate receptors

Jia-Hua Hu[1], **Linlin Yang**[1], **Paul J Kammermeier**[2], **Chester G Moore**[1], **Paul R Brakeman**[1,7], **Jiancheng Tu**[1], **Shouyang Yu**[3], **Ronald S Petralia**[4], **Zhe Li**[1], **Ping-Wu Zhang**[1], **Joo Min Park**[1], **Xinzhong Dong**[1,5], **Bo Xiao**[1,3], and **Paul F Worley**[1,6]

[1]Solomon H. Snyder Department of Neuroscience, Johns Hopkins University School of Medicine, Baltimore, Maryland, USA

[2]Department of Pharmacology and Physiology, University of Rochester Medical Center, Rochester, New York, USA

[3]The State Key Laboratory of Biotherapy, West China Hospital, Sichuan University, Chengdu, China

[4]National Institute on Deafness and Other Communication Disorders, US National Institutes of Health, Bethesda, Maryland, USA

[5]Howard Hughes Medical Institute, Johns Hopkins University School of Medicine, Baltimore, Maryland, USA

[6]Department of Neurology, Johns Hopkins University School of Medicine, Baltimore, Maryland, USA

Abstract

Group I metabotropic glutamate receptors (mGluRs), including mGluR1 and mGluR5, are G protein–coupled receptors (GPCRs) that are expressed at excitatory synapses in brain and spinal cord. GPCRs are often negatively regulated by specific G protein–coupled receptor kinases and subsequent binding of arrestin-like molecules. Here we demonstrate an alternative mechanism in which group I mGluRs are negatively regulated by proline-directed kinases that phosphorylate the binding site for the adaptor protein Homer, and thereby enhance mGluR–Homer binding to reduce signaling. This mechanism is dependent on a multidomain scaffolding protein, Preso1, that binds

Correspondence should be addressed to P.F.W. (pworley@jhmi.edu).
[7]Present address: Department of Pediatrics, University of California, San Francisco, San Francisco, California, USA.

Supplementary information is available in the online version of the paper.

COMPETING FINANCIAL INTERESTS

The authors declare no competing financial interests.

AUTHOR CONTRIBUTIONS

J.-H.H. designed, performed and analyzed experiments included in Figures 1–7 and Supplementary Figures 1–6 and 8, and wrote a first draft of the manuscript. L.Y. performed and analyzed experiments in Figures 1 and 2 and Supplementary Figure 4. P.J.K. performed and analyzed electrophysiology experiments in Figure 3. C.G.M. generated and identified the phospho-mGluR antibody in Supplementary Figure 4. P.R.B. performed the yeast-two hybrid screen that identified Preso1 as a Homer binding protein. J.T. and B.X. cloned Preso1 and did initial characterizations. S.Y. generated the Preso1 antibody. R.S.P. performed the experiments in Figure 1. Z.L. performed and analyzed experiments in Supplementary Figure 7. P.-W.Z. generated *Grm5*$^{R/R}$ mice. J.M.P. performed electrophysiological experiments. X.D. provided intellectual input and technical support on the behavioral experiments and dorsal root ganglion neuron recordings. B.X. generated Preso1 antibodies, designed and performed experiments in Figure 1 and provided intellectual input and technical support for *Preso1*$^{-/-}$ mouse generation. P.F.W. supervised the overall project, designed experiments and wrote the final version of the manuscript.

mGluR, Homer and proline-directed kinases and that is required for their phosphorylation of mGluR at the Homer binding site. Genetic ablation of Preso1 prevents dynamic phosphorylation of mGluR5, and *Preso1*$^{-/-}$ mice exhibit sustained, mGluR5-dependent inflammatory pain that is linked to enhanced mGluR signaling. Preso1 creates a microdomain for proline-directed kinases with broad substrate specificity to phosphorylate mGluR and to mediate negative regulation.

Group I metabotropic glutamate receptors (mGluRs) are enriched at excitatory synapses in the brain, where they are important in neural plasticity[1] and behavioral responses including inflammatory pain, fear conditioning, drug addiction and schizophrenia[2–4]. Group I mGluRs localize primarily to the lateral margin of the post-synaptic membrane[5], where they respond to glutamate as it diffuses from release sites in the central synaptic region[6]. Group I mGluRs evoke changes by modulating membrane ion channels[7], intracellular ion channels[8] and signaling cascades including EF2 kinase[9], MAP kinase[10], mTORC1 (ref. 11) and endocannabinoid synthesis[12]. The coupling mechanisms for several of these outputs involve proteins of an adaptor protein family, termed Homer, that bind to a proline-rich sequence in the C terminus of group I mGluRs[13]. In an exemplar assay, Homer binding to group I mGluRs expressed in superior cervical ganglion neurons blocks coupling to M-type potassium channels and voltage sensitive Ca^{2+} channels[7]. Homer binding to group I mGluRs also reduces agonist-independent activation of BK channels in granule cell neurons[14].

The Homer binding site (TPPSPF) contains a consensus site for proline-directed kinases. Proline-directed kinases are activated by multiple neurotransmitter and growth factor receptors and are critical in the control of cellular processes including cell proliferation, differentiation, motility and neuronal plasticity[15]. The ability of Homer binding to modify mGluR signaling begs the question of whether proline-directed kinase–mediated phosphorylation of mGluR functions in receptor signaling.

Here we report that group I mGluR signaling is dynamically controlled by proline-directed kinases acting in concert with a multi-domain scaffolding protein termed Preso1. Preso1 includes WW, PDZ and FERM domains, and it was previously reported to bind PSD95 (ref. 16) and to modulate dendritic spine morphogenesis. We identified Preso1 in a screen for proteins that bind Homer and determined that it also binds group I mGluR and proline-directed kinases including CDK5 and ERK. Preso1 enhances the ability of proline-directed kinases to bind mGluR and phosphorylate the Homer binding site in mGluR. This action of Preso1 appears analogous to that of A-kinase anchoring proteins (AKAPs)[17] to recruit PKA to phosphorylate its substrates. Preso1-dependent phosphorylation of mGluR enhances Homer binding and downregulates mGluR signaling in cellular assays. To assess this mechanism *in vivo*, we examined behavioral responses in a mouse model of inflammatory pain, which is dependent on sustained activation of group I mGluRs[3]. We confirmed that inflammatory pain depended on mGluR5 and was increased in mouse models that interrupt Homer binding to mGluR5, owing either to genetic deletion of Homer or to genetic knock-in of an mGluR5 point mutant that cannot bind Homer. Inflammatory pain was also increased in a *Preso1*$^{-/-}$ mouse, and this was coupled to increased mGluR5 activity. These studies support a model in which Preso1 functions to facilitate proline-directed kinase modulation of Homer binding to mGluR and thereby controls the amplitude and duration of mGluR signaling.

RESULTS

Preso1 is a Homer-binding protein enriched in brain

We used the Homer1 EVH1 domain to perform a yeast two-hybrid screen of a rat brain cDNA library and identified a 1.2-kb fragment corresponding to the C terminus of

KIAA0316. The full-length gene was cloned by 5′ and 3′ rapid amplification of cDNA ends (RACE) and determined to be homologous to human *FRMPD4* (also termed *PDZD10*, *PDZK10* and *Preso*[16]), and is here termed *Preso1*. The Preso1 protein contains several domains, including a Homer binding site (Fig. 1a), and is conserved from *Drosophila melanogaster* to human (Supplementary Fig. 1). Public databases include two related genes that we term *Preso2* (*FRMPD3*, *KIAA1817*) and *Preso3* (*FRMPD1* (ref. 18), *FRMD2*, *KIAA0967*) (Supplementary Fig. 2). Mouse and human *Preso1* and *Preso2* are near each other on the X chromosome, whereas *Preso3* is autosomal (human chromosome 9, mouse chromosome 4). mRNAs of all three *Preso* genes are expressed broadly in brain and spinal cord in mouse (Supplementary Fig. 3).

Hemagglutinin (HA)-tagged Homer1c (the brain-enriched Homer1 splice form)[19] immunoprecipitated with Preso1 (Fig. 1b). This interaction was disrupted either by point mutation of the canonical polyproline-binding surface of the Homer1 EVH1 domain or by point mutation of the predicted Homer binding site in Preso1 (Preso1FR; Fig. 1b). Thus, the Homer–Preso1 interaction involves conventional binding properties of Homer, and it seems to be direct. Preso2 encodes a conserved Homer binding site, and it immunoprecipitated with Homer1c from HEK293T cell lysates, whereas Preso3 lacks a conserved Homer binding site and did not coimmunoprecipitate (Supplementary Fig. 4a).

To examine the association of Preso1 with Homer *in vivo*, we immunoprecipitated Preso1 from detergent lysates of rat cerebellum and confirmed that Homer3 was coimmunoprecipitated (Fig. 1c). mGluR1 and components of its signaling complex, including Shank, PSD95 and the inositol-1,4,5-trisphosphate receptor (IP_3R) also immunoprecipitated with Preso1 (Fig. 1c). Preso1 immunoreactivity was enriched in cultured hippocampal neurons and showed a punctate distribution that colocalized with the excitatory synaptic marker PSD95, but not with the inhibitory synaptic marker glutamic acid decarboxylase (GAD65) (78.6 ± 4.8% of Preso1 colocalized with PSD95 (all values expressed as ± 95% confidence interval), whereas 9.6 ± 2.1% colocalized with GAD65; n = 17–20 dendrites in 7 or 8 neurons; Fig. 1d). Preso1 immunoreactivity also colocalized with mGluR5 in the neurons (68.6 ± 5.1%; Fig. 1d). To confirm that Preso1 is a synaptic protein, we performed immunogold electron microscopy in the hippocampus. Preso1-immunogold localized to the postsynaptic spine, especially in the PSD and subjacent cytoplasm, overlapping the distributions of Homer and group I mGluRs[5,19] (Fig. 1e).

Preso1 interacts with group I mGluRs via its FERM domain

We considered the possibility that Preso1 functions as a scaffolding protein for group I mGluRs. Consistent with brain coimmunoprecipitation data, Preso1 immunoprecipitated with mGluR5 from detergent lysates of HEK293T cells (Fig. 2a and Supplementary Fig. 4b). By contrast, Preso1 did not immunoprecipitate mGluR2 or mGluR4, which belong to group II and group III mGluRs (Supplementary Fig. 4c, d). Preso1 possesses several protein interaction domains, and we examined whether Preso1 might directly interact with mGluR5 independent of Homer. Preso1 or deletion mutants were cotransfected with HA-tagged mGluR5 into HEK293T cells and assayed for interaction by coimmunoprecipitation. Preso1 antibody immunoprecipitated mGluR5 that was expressed with any of the N-terminal deletion mutants except Preso1-ΔFERM (Fig. 2a). Notably, point mutants of both Preso1 and mGluR5 that do not bind Homer (Preso1FR; $mGluR5_{F1128R}$ (mGluR5FR)) retained interaction in the coimmunoprecipitation assay (Fig. 2a), suggesting that Preso1 binding to mGluR5 does not depend on Homer. These data also suggest that the FERM domain is required for Preso1 binding to mGluR5. We confirmed that the isolated Preso1 FERM domain was sufficient to immunoprecipitate mGluR5 (Fig. 2b).

We next examined the region of mGluR5 required for interaction with Preso1 using coimmunoprecipitation assays with mGluR5 C-terminal mutants. Preso1 immunoprecipitated $mGluR5_{1–1020}$, but not $mGluR5_{1–920}$ (Fig. 2c). As the Homer binding site is at 1128, these data indicate that sequence element(s) in mGluR5 required for Preso1 binding are at least 100 amino acids remote from the Homer binding site (Fig. 2d). $mGluR5_{920–1020}$ includes a predicted FERM domain binding site[20] and a D-domain implicated as a binding site for proline-directed kinases in other proteins[21] (Fig. 2d). Mutations of the putative FERM domain binding sites ($mGluR5_{Y965A\ V967A}$) resulted in only a modest reduction of its immunoprecipitation with Preso1 (Fig. 2e). However, the combined point mutations of the putative FERM-binding site and the Homer binding site ($mGluR5_{Y965A\ V967A\ F1128R}$; mGluR5YVF) markedly reduced mGluR5 immunoprecipitation with Preso1 (Fig. 2e). The dependence of mGluR5–Preso1 binding on the Homer binding site in mGluR5 is consistent with the notion that native Homer proteins in HEK293T cells[22] can link these proteins, and it suggests that Preso1 binding to mGluR involves contributions of both the FERM domain–binding site and the Homer binding site.

Preso1 regulates mGluR phosphorylation and signaling

Coexpression of Preso1 increased binding between Homer and mGluR5 (172.7 ± 29.4% of control, $n = 6$, $P = 0.004$; Fig. 3a). As Homer binding can be increased by phosphorylation of mGluR5 at the Homer binding site[23], we hypothesized that Preso1 might function to increase Homer binding by increasing mGluR5 phosphorylation. We developed a phospho-specific antibody to the Homer binding site of group I mGluR (Supplementary Fig. 4e), and found that mGluR5 phosphorylation increased with Preso1 expression (198.2 ± 72.8% of control, $n = 7$; $P = 0.04$; Fig. 3a). To exclude the possibility that Preso1 increases Homer–mGluR5 binding indirectly by means of the association of Preso1 with Homer, we confirmed Preso1's effect using a mutant (Preso1FR) that does not bind Homer (Fig. 1b). Enhanced Homer binding is dependent on phosphorylation, as Preso1 did not enhance Homer binding to an mGluR mutant (mGluR5TSAA, containing TS to AA mutations at Homer binding site) that cannot be phosphorylated at the Homer site (mGluR5 wild type (WT): 183.7 ± 51.8% of control, $n = 6$; $P = 0.03$; mGluR5TSAA: 122.6 ± 49.1% of control, $n = 6$; $P = 0.58$; Fig. 3b). These data suggest that mGluR5 phosphorylation at its Homer binding site mediates Preso1's effect of increasing Homer binding to mGluR5.

We next investigated whether Preso1 regulates group I mGluR function. In a cellular assay, group I mGluR coupling to voltage-sensitive calcium channels in superior cervical ganglion neurons, which do not natively express any mGluRs[24], was inhibited by Homer binding[7] and was similarly inhibited by Preso1 (mGluR1: 55 ± 6% in control, $n = 15$; 16 ± 8% in Preso1, $n = 11$; $P = 0.0001$; mGluR5: 38 ± 5% in control, $n = 24$; 22 ± 6% in Preso1, $n = 22$; $P = 0.0004$; Fig. 3c,d). Experiments with mGluR5 mutants indicated that Preso1's action depended on Preso1 binding to mGluR5 (absent with mGluR5YVF), Homer binding to mGluR5 (absent with mGluR5FR) and phosphorylation of the Homer binding site in mGluR5 and mGluR1 (absent with mGluR5TSAA and mGluR1TSAA) (mGluR5YVF: 26 ± 10% in control, $n = 7$; 25 ± 6% in Preso1, $n = 8$, $P = 0.90$; mGluR5FR: 26 ± 10% in control, $n = 7$; 23 ± 10% in Preso1, $n = 11$, $P = 0.66$; mGluR5TSAA: 16 ± 10% in control, $n = 9$; 16 ± 6% in Preso1, $n = 13$, $P = 0.98$; mGluR1TSAA: 43 ± 12% in control, $n = 14$; 41 ± 16% in Preso1, $n = 6$, $P = 0.88$; Fig. 3d). Preso1 action is specific for group I mGluR, as it did not alter the activity of mGluR2 (64 ± 4% in control, $n = 7$; 57 ± 12% in Preso1, $n = 5$, $P = 0.30$; Fig. 3d), consistent with the finding that Preso1 selectively bound group I mGluRs (Supplementary Fig. 4b–d).

Preso1 binds proline-directed kinases

Inspection of the Homer binding site of group I mGluR (Fig. 2d) suggested that the serine phosphorylation is mediated by proline-directed kinases, such as CDK5 and ERK. We found that expression of CDK5 and p35 (CDK5/p35) or constitutively active MEK (MEK DD), which activates ERK, induced mGluR5 phosphorylation in HEK293T cells (CDK5/p35: 563 ± 98% of control, $n = 6$; $P = 0.0008$; MEK DD: 1,049 ± 345% of control, $n = 6$; $P = 0.006$; Fig. 4a). In cultured neurons, native mGluR phosphorylation was significantly reduced by CDK5 inhibitor or MEK inhibitor (UO126: 57.4 ± 11% of untreated, $n = 4$; $P = 0.007$; purvalanol A: 65.8 ± 9.5% of untreated, $n = 4$; $P = 0.02$; Fig. 4b). These data support a role for CDK5 and ERK in phosphorylation of group I mGluR at the Homer binding site.

We next hypothesized that Preso1 binds proline-directed kinases that phosphorylate group I mGluRs. Preso1 contains a predicted D-domain that is conserved among Preso family members and across species (Supplementary Figs. 1 and 2). As predicted, Preso1 immunoprecipitated from HEK293T cells with proline-directed kinases CDK5 and ERK (Fig. 4c,d). Additionally, Preso1 enhanced the association of ERK1 with mGluR5 in HEK293T cells (166.6 ± 40% of control, $n = 5$; $P = 0.02$; Fig. 4e). Endogenous Preso1 immunoprecipitated with CDK5 and with ERK1 and/or ERK2 (ERK1/2) from mouse brain (Fig. 4f,g), suggesting that Preso1 and proline-directed kinases are naturally associated *in vivo*.

Preso1$^{-/-}$ mouse generation

We generated a conditional *Preso1*$^{-/-}$ by inserting *lox*P sites in flanking introns of exon 3, which encodes the PDZ domain (Supplementary Fig. 5a). Preso1 was deleted in the germline by mating conditional knockout mice with *CMV-cre* mice. *Preso1*$^{-/-}$ mice were identified by PCR (data not shown), and mutant Preso1 mRNA expression was confirmed by reverse transcription and PCR of cortex and cerebellum (Supplementary Fig. 5b). Preso1 deletion was further verified by western blots of detergent lysates of *Preso1*$^{-/-}$ brain (Supplementary Fig. 5c) and cultured cortical neurons (Supplementary Fig. 5d). Male and female *Preso1*$^{-/-}$ mice were viable and fertile, and appear similar to WT mice in their post-natal growth. Expression of Homer1b/c, Homer2, Homer3, NR1, GluA1 and GluA2/3 was not altered in 6-week-old *Preso1*$^{-/-}$ brain, and expression of mGluR5 was not different in cortex or spinal cord (Supplementary Fig. 5e).

Consistent with the hypothesized function of Preso1, mGluR5 phosphorylation (pSer-mGluR) and mGluR5 immunoprecipitation with Homer was reduced in *Preso1*$^{-/-}$ cortex and spinal cord compared those in to WT littermates (binding: 76 ± 3.3% of WT in cortex, $n = 5$; $P = 0.002$; 73.6 ± 8.7% of WT in spinal cord, $n = 8$; $P = 0.03$; phosphorylation: 57.5 ± 22.2% of WT in cortex, $n = 5$; $P = 0.04$; 79.1 ± 10.6% of WT in spinal cord, $n = 5$; $P = 0.03$; Fig. 5a). Additionally, immunoprecipitation of ERK1/2 with mGluR5 was reduced in *Preso1*$^{-/-}$ brain (64.4 ± 10.9% of WT, $n = 5$; $P = 0.04$; Fig. 5b).

Preso1 is required for dynamic Homer–mGluR5 binding

We examined the hypothesis that Preso1 is required for activity-dependent phosphorylation of mGluR5 and enhanced Homer binding. In WT neurons, the group I mGluR agonist 3,5-dihydroxyphenyl-glycine (DHPG) resulted in an increase of mGluR5 phosphorylation and Homer binding to mGluR5 after 30 min (binding: 157 ± 33.8% of untreated, $n = 5$; $P = 0.01$; phosphorylation: 149 ± 36% of untreated, $n = 5$; $P = 0.02$; Fig. 5c). By contrast, mGluR5 phosphorylation and Homer binding were reduced in *Preso1*$^{-/-}$ neurons and were not changed after DHPG stimulation (binding: 47 ± 7.7% in untreated *Preso1*$^{-/-}$, $n = 5$; $P = 0.007$; 54 ± 12.9% in treated *Preso1*$^{-/-}$, $n = 3$; $P = 0.3$; phosphorylation: 71.7 ± 22.4% in untreated *Preso1*$^{-/-}$, $n = 5$; $P = 0.04$; 67.3 ± 14.8% in treated *Preso1*$^{-/-}$, $n = 5$; $P = 0.76$; Fig.

5c). This is consistent with mGluR5 activation of CDK5 and ERK[25], which then phosphorylate the receptor to mediate enhanced Homer binding in a receptor homologous feedback pathway. We also examined the effect of BDNF, which activates TrkB to increase ERK[26], and found similar increases of mGluR5 phosphorylation and Homer binding in WT but not *Preso1*$^{-/-}$ neurons (binding: 157.7 ± 14.5% in treated WT, $n = 4$; $P = 0.001$; 65.3 ± 18% in untreated *Preso1*$^{-/-}$, $n = 4$; $P = 0.02$; 69.8 ± 22.9% in treated *Preso1*$^{-/-}$, $n = 4$; $P = 0.77$; phosphorylation: 182.1 ± 15.1% of untreated, $n = 5$; $P = 0.00002$; 66.8 ± 9.5% in untreated *Preso1*$^{-/-}$, $n = 4$; $P = 0.0002$; 79.7 ± 8.3% in treated *Preso1*$^{-/-}$, $n = 4$; $P = 0.09$; Fig. 5c). These observations suggest that Preso1 is required for dynamic regulation of mGluR5 phosphorylation and Homer binding in both homologous and heterologous receptor signaling pathways.

Tamalin[27], calcineurin inhibitor protein (CAIN)[28] and Norbin[29] bind group I mGluRs and modify signaling by changing expression of mGluR on the cell surface. mGluR5 expression on the surface of neurons in culture was not different between WT and *Preso1*$^{-/-}$ (115.6 ± 21.6% of WT, $n = 6$; $P = 0.14$; Fig. 5d). Furthermore, DHPG induced identical decreases of surface mGluR5 (65.4 ± 16.7% in WT, $n = 4$; $P = 0.02$; 65.2 ± 10.1% in *Preso1*$^{-/-}$, $n = 3$; $P = 0.04$; Fig. 5d), suggesting that Preso1 does not function by regulating mGluR5 surface expression. This is consistent with the observed absence of an effect of *Homer1*$^{-/-}$*Homer2*$^{-/-}$ *Homer3*$^{-/-}$ genotype on mGluR5 surface expression[30].

Pain response is increased in *Preso1*$^{-/-}$ mice

Formalin injection into the mouse hind paw results in an initial, transient behavioral pain response that is followed by a second, sustained response that is associated with tissue inflammation and is termed inflammatory pain[31]. This model is widely used in pain research, and group I mGluRs have been implicated in inflammatory pain by means of pharmacological agonists and antagonists[3]. To further validate the role of mGluR5, we examined *Grm5*$^{-/-}$ mice and confirmed decreased pain responses in the second phase, but not in the first phase, after formalin injection compared with responses in their WT littermates (Supplementary Fig. 6a,b). Furthermore, 2-methyl-6-(phenylethynyl)-pyridine (MPEP), an mGluR5 specific antagonist, substantially reduced the formalin-induced inflammatory pain response in WT mice, but not in *Grm5*$^{-/-}$ mice (Supplementary Fig. 6a,b). These results confirm a role for mGluR5 in formalin-induced inflammatory pain.

We next asked whether formalin-induced inflammatory pain is altered in *Preso1*$^{-/-}$ mice. *Preso1*$^{-/-}$ mice exhibited greater behavioral pain responses during the second phase, but not the first phase, compared with their WT littermates (first phase: 94.6 ± 24.2 s in WT, $n = 9$; 88 ± 25 s in *Preso1*$^{-/-}$, $n = 8$; $P = 0.72$; second phase: 347.6 ± 52.8 s in WT, $n = 9$; 576.3 ± 113.2 s in *Preso1*$^{-/-}$, $n = 8$; $P = 0.002$; Fig. 6a,b). Notably, MPEP (30 mg per kilogram body weight, intraperitoneally) decreased pain responses during the second phase to the same degree in *Preso1*$^{-/-}$ and WT mice (first phase: 68.7 ± 11.7 s in treated WT, $n = 6$; $P = 0.13$; 76.8 ± 24.7 s in treated *Preso1*$^{-/-}$, $n = 6$; $P = 0.56$; second phase: 207 ± 33.5 s in treated WT, $n = 6$; $P = 0.002$; 214.7 ± 47.3 s in treated *Preso1*$^{-/-}$, $n = 6$; $P = 0.0002$; Fig. 6a,b). These data indicate that the increased inflammatory pain response in *Preso1*$^{-/-}$ is mediated by mGluR5. Because ongoing sensory inputs contribute to formalin-induced pain[32], we measured the excitability of dorsal root ganglion neurons from WT and *Preso1*$^{-/-}$ mice and found similar excitabilities (Supplementary Fig. 7). To assess the notion that Homer binding to mGluR5 is important to limit the intensity of the inflammatory pain response, we confirmed that inflammatory pain behavior was increased in *Homer2*$^{-/-}$*Homer3*$^{-/-}$ mice, and in an mGluR5 mutant knock-in mouse in which Homer cannot bind the receptor (*Grm5*$^{R/R}$ or mGluR5FR mice[33]) (Supplementary Fig. 8a–d). Furthermore, we found that inflammatory pain behavior was decreased in mice with selective deletion of the *Homer1a*

isoform of the *Homer1* gene (*Homer1a*$^{-/-}$ mice)[30] (Supplementary Fig. 8e,f), consistent with a mechanism whereby deletion of Homer1a increases Homer binding with mGluR5.

c-Fos expression is induced in neurons of the lumbar dorsal spinal cord by formalin injection into the hind paw, and it identifies neurons activated in the pain circuit that increase cellular [Ca^{2+}][34]. We performed c-Fos immunostaining in lumbar level L4–L5 spinal cord from WT and *Preso1*$^{-/-}$ mice after formalin injection and found more c-Fos positive neurons in the *Preso1*$^{-/-}$ spinal cord than in WT spinal cord (lamina 1–2: 19.6 ± 2.7 in WT, $n = 25$; 26.6 ± 4.1 in *Preso1*$^{-/-}$, $n = 22$; $P = 0.007$; lamina 3–4: 6.1 ± 1.0 in WT, $n = 25$; 8.7 ± 2.1 in *Preso1*$^{-/-}$, $n = 18$; $P = 0.03$; lamina 5–6: 5.8 ± 1.1 in WT, $n = 25$; 11.1 ± 2.4 in *Preso1*$^{-/-}$, $n = 18$; $P = 0.0001$; Fig. 6c,d). Furthermore, preinjection with MPEP reduced the number of c-Fos–positive neurons in the WT and *Preso1*$^{-/-}$ spinal cord to the same degree (lamina 1–2: 14.9 ± 2.8 in treated WT, $n = 18$; $P = 0.03$; 13.6 ± 2.22 in treated *Preso1*$^{-/-}$, $n = 18$; $P = 0.000009$; lamina 3–4: 3.7 ± 0.7 in treated WT, $n = 18$; $P = 0.001$; 5.2 ± 0.8 in treated *Preso1*$^{-/-}$, $n = 18$; $P = 0.009$; lamina 5–6: 6.2 ± 1.2 in treated WT, $n = 18$; $P = 0.62$; 7.8 ± 1.2 in treated *Preso1*$^{-/-}$, $n = 18$; $P = 0.03$; Fig. 6c,d). These findings corroborate behavioral pain assays and suggest that *Preso1*$^{-/-}$ increases the number of neurons in the spinal cord pain pathway that reach a critical level of [Ca^{2+}] for c-Fos induction, through a mGluR5-dependent mechanism.

We also tested pain responses in the complete Freund's adjuvant (CFA) chronic pain model. *Preso1*$^{-/-}$ mice were not different from WT littermates in their basal thermal pain responses, and they showed an identical initial pain response (WT: 13.6 ± 2.2 s, $n = 9$; *Preso1*$^{-/-}$: 13.6 ± 3.3 s, $n = 9$; $P = 0.96$; Fig. 6e). However, *Preso1*$^{-/-}$ mice exhibited increased thermal pain responses beginning 3 d after CFA injection and persisting through 5 d (day 1: 6.9 ± 2.1 s in WT, $n = 9$; 6.6 ± 2.6 s in *Preso1*$^{-/-}$, $n = 9$; $P = 0.83$; day 2: 10.2 ± 5.0 s in WT, $n = 9$; 7.3 ± 5.5 s in *Preso1*$^{-/-}$, $n = 9$; $P = 0.26$; day 3: 11.7 ± 3.6 s in WT, $n = 9$; 7.5 ± 3.3 s in *Preso1*$^{-/-}$, $n = 9$; $P = 0.02$; day 4: 11.1 ± 2.9 s in WT, $n = 9$; 2.6 ± 2.4 s in *Preso1*$^{-/-}$, $n = 9$; $P = 0.03$; day 5: 13.6 ± 4.2 s in WT, $n = 9$; 9.9 ± 2.2 s in *Preso1*$^{-/-}$, $n = 9$; $P = 0.03$; Fig. 6e).

Enhanced mGluR-mediated Ca^{2+} response in *Preso1*$^{-/-}$ neurons

Preso1 is expressed in the dorsal spinal cord (Supplementary Fig. 3) with an expression pattern similar to mGluR5[35]. On the basis of the increased behavioral pain and c-Fos expression in spinal cord of *Preso1*$^{-/-}$ mice, we predicted that group I mGluR function would be enhanced in *Preso1*$^{-/-}$ dorsal spinal cord neurons. We cultured these neurons from WT and *Preso1*$^{-/-}$ mice and performed calcium imaging assays. Glutamate (100 μM) combined with APV (100 μM), an NMDA receptor blocker, and NBQX (100 μM), an AMPA receptor blocker, were used to stimulate mGluR. This cocktail was found to be more consistent than a selective agonist for mGluR5 (DHPG), as is consistent with the observation that mGluR1 signaling is enhanced by preceding depolarization[36]. Stimulation induced a rise of [Ca^{2+}] in both WT and *Preso1*$^{-/-}$ neurons that persisted until washout (Fig. 7a). The calcium response in *Preso1*$^{-/-}$ neurons was significantly greater than that in WT neurons (WT: 3.28 ± 0.33 fold increase over basal Ca^{2+}, $n = 90$; *Preso1*$^{-/-}$: 4.47 ± 0.44 fold increase over basal Ca^{2+}, $n = 74$; $P = 0.00003$; Fig. 7a). Pretreatment with MPEP (10 μM) and with Bay36-7620 (20 μM), an mGluR1 antagonist, blocked the sustained calcium response (Fig. 7a), confirming that it is dependent on group I mGluR.

We next asked whether the enhanced mGluR-mediated calcium response in *Preso1*$^{-/-}$ spinal cord neurons would be rescued by expressing a *Preso1* transgene. GFP or GFP-Preso1 constructs were electroporated into dorsal spinal cord neurons from *Preso1*$^{-/-}$ mice on the day of culture initiation and used for calcium imaging after 2 d. GFP-Preso1–expressing neurons showed a markedly reduced mGluR-mediated calcium response compared to GFP expressing neurons (GFP: 2.38 ± 0.36 fold increase over basal Ca^{2+}, $n = 23$; GFP-Preso1:

0.46 ± 0.35 fold increase over basal Ca^{2+}, $n = 19$; $P = 5 \times 10^{-9}$; Fig. 7b), indicating that increased Ca^{2+} responses in *Preso1*$^{-/-}$neurons can be reversed by Preso1.

Our model predicts that Preso1 facilitates proline-directed kinases to increase mGluR phosphorylation at the Homer binding site, and inhibits sustained mGluR responses (Fig. 4). Accordingly, we asked whether the mGluR-dependent Ca^{2+} response in spinal cord neurons is altered by proline-directed kinase inhibitors. We observed that the Ca^{2+} response to sustained treatment with glutamate, APV and NBQX decreased over an interval of 2–9 min in most neurons, but [Ca^{2+}] again increased until washout in some neurons (Fig. 7c). The percentage of neurons with Ca^{2+} rise was significantly higher in *Preso1*$^{-/-}$ than that in WT (WT: 11.5 ± 4.3%, $n = 390$; *Preso1*$^{-/-}$: 22.3 ± 7.4%, $n = 360$; $P = 0.03$; Fig. 7c). The reversal by washout and subsequent cell viability assessed by Nomarski microscopy indicated that the delayed response was not due to cell death. Addition of UO126 (4 μM), or purvalanol A (5 μM) 2 min after onset of stimulation resulted in a two- to threefold increase of the percentage of neurons exhibiting a delayed rise of [Ca^{2+}] (UO126: 28.3 ± 5.7%, $n = 420$; $P = 0.0004$; purvalanol A: 23.8 ± 5.6%, $n = 330$; $P = 0.005$; Fig. 7c). By contrast, kinase inhibitors did not change the percentage of *Preso1*$^{-/-}$ spinal cord neurons showing this delayed response (UO126: 27.6 ± 6.6%, $n = 270$; $P = 0.32$; purvalanol A: 25.0 ± 5.3%, $n = 190$; $P = 0.60$; Fig. 7c). Although kinase inhibitors are likely to alter multiple signaling pathways, their acute action in blocking mGluR-dependent increases of [Ca^{2+}] is consistent with our model of Preso1 function.

DISCUSSION

The present study indicates that Preso1 functions as an essential part of the group I mGluR signaling complex, and supports its role as an anchoring protein for proline-directed kinases that mediate activity- dependent, negative regulation of mGluR. The Preso1–proline-directed kinase–Homer mechanism is highly dynamic, and findings support a consistent model across biochemical and behavioral phenotypes in several genetic models that modify Homer expression or Homer binding to mGluR. This mechanism is distinct from the canonical mechanism of GPCR desensitization mediated by G protein– coupled receptor kinases and β-arrestin pathway[37] in several ways. First, Preso1 and dynamic Homer binding do not influence the level of surface mGluR expression either in steady state conditions or after activation of the mGluR receptor. Inhibition of mGluR signaling appears to result as a direct consequence of Homer binding rather than of removal from the plasma membrane. Second, the proline-directed kinases that mediate this response are not specific for the receptor, but rather are activated by many signaling pathways. This affords the possibility of receptor crosstalk, but it also highlights the importance of an anchoring protein for mGluR that can confer specificity to broad-substrate proline-directed kinases and thereby mimic the intrinsic specificity of G protein–coupled receptor kinases. Group I mGluRs reportedly desensitize in response to G protein–coupled receptor kinases[38], but the natural relevance of the suggested pathways remains unknown. The Preso1 mechanism is distinct from other proteins that bind group I mGluR and modify signaling by changing expression of mGluR on the cell surface, including Tamalin[27], calcineurin inhibitor protein (CAIN)[28] and Norbin[29].

Preso1 appears to limit the amplitude and duration of mGluR5 activation that underlies inflammatory pain in the formalin model and chronic pain in the CFA model. Preso1-dependent inhibition of mGluR5 may occur normally as part of a homologous receptor down-regulation due to increased mGluR5 activation by glutamate, or as a heterologous receptor response due to increased proline-directed kinase activation by receptors such as TrkB[26] or the bradykinin receptor[39]. Phosphorylated ERK is upregulated during inflammatory pain and has been implicated as a mediator of neuronal excitability due to

phosphorylation of a potassium channel[40]. CDK5 expression and activity is also elevated during inflammation and regulates pain signaling[41]. Previous studies have demonstrated that group I mGluR signaling becomes agonist independent if Homer does not bind and crosslink the receptor[14]. This mechanism underlies the effect of Homer1a in driving homeostatic scaling of AMPA receptors[30] and has been suggested to contribute to stress effects in fear conditioning[42]. Accordingly, agonist- independent mGluR5 signaling may contribute to inflammatory pain. Pain induced by inflammation also causes central sensitization and hypersensitivity[43], and recent studies suggest a special role for the amygdala[44]. Hence, it is possible that Preso1 also contributes to central sensitization through regulation of mGluR function.

Group I mGluRs are important targets for therapies of cognitive diseases including fragile X mental retardation syndrome[45] and Alzheimer's disease[5], and are notable for the ability of pharmacological agents to differentially alter signaling outputs (biased ligands)[46]. It is possible that Preso1 contributes to this distinctive pharmacology. Although Preso1 and Homer binding uniformly inhibited the responses of group I mGluRs monitored here, group I mGluRs signal in several output pathways (see introduction), and Homer binding to mGluR5 does not uniformly inhibit all outputs. For example, mGluR1 coupling to intracellular IP_3 receptors is increased by Homer crosslinking[47]. Accordingly, the effect of Preso1 on the signaling of group I mGluRs could be output specific.

The yeast protein STE5 provides a precedent for a proline-directed kinase anchoring protein[48], but Preso1 appears to be the first example of a proline-directed kinase anchoring protein for higher organisms. This action is similar to that of AKAPs, which coordinate signal transduction complexes by recruiting multiple signaling enzymes near potential substrates, including G protein–coupled receptors[49]. Consistent with the notion that Preso1 functions as an anchoring protein, Preso1 includes domains that can interact with the cytoskeleton, including the Rac-activation domain, and has been reported to interact with β-Pix[16]. Many GPCRs encode predicted FERM domain binding sites and D-domains (GPCR databases; http://www.gpcr.org/7tm/), suggesting that Preso family members may have a broader role in GPCR signaling. However, only group I mGluRs contain a Homer binding site that is also a consensus for proline-directed kinases, which predicts that Presos uniquely coordinate dynamic changes of Homer binding to group I mGluR. Preso2 and Preso3 mRNAs are broadly expressed in the nervous system, but they have not been examined for their role in regulating GPCR signaling. Presos are also expressed outside of the central nervous system[18], and they will be important for a comprehensive understanding of GPCR signaling.

ONLINE METHODS

Expression constructs

All the expression constructs were made by PCR. Internal deletions and point mutations were made either using QuikChange Site-Directed Mutagenesis Kit (Stratagene) or by megaprimer method. The sequence for each mutant will be supplied upon request. PCR products were cloned into expression vectors pEGFPC1 (Clontech), pGEX 4T2 (Pharmacia), and pRK5 (Genentech), with Myc or HA tags. All constructs were verified by sequencing.

Antibodies

Preso1 antibodies were generated in rabbits using the rat Preso1 C terminal 20 aa or 330 aa as antigens. The antibody from 20-aa antigen was used for immunoelectron microscopy (1:100), and the antibody from 330-aa antigen was used for western blot (1:2,000) and immunostaining (1:100). Group I mGluR phospho-Ser antibody was generated in two

female rabbits using rat mGluR5 peptide (ELVALTPPpSPFRD) as antigen (1:3,000 for western blot). These rabbit antibodies were generated by Covance, except the Preso1 antibody against the 330-aa antigen, which was generated at Sichuan University under a rabbit protocol approved by Animal Care and Use Committee of Sichuan University. All other antibodies were previously described or were acquired commercially, and their dilutions are as follows: mGluR5 (Upstate, 06-451) at 1:10,000, mGluR1 (BD, 610965) at 1:10,000, IP_3R (gift from Alan Sharp (Johns Hopkins University School of Medicine)) at 1:1,000, Shank (Neuromab, clone N23B/49) at 1:2, PSD95 (Neuromab, clone K28/43) at 1:5,000, GluA1 (JH1710) at 1:1000, GluA2 (JH1707) at 1:500, NR1 (Millipore, 05-432) at 1:1,000, pan-Homer (Santa Cruz, sc-17842) for immunoprecipitation, Homer1 (JH2621) at 1:5,000, Homer2 (JH2623) at 1:5,000, Homer3 (JH2793) at 1:5,000, ERK (Cell Signaling, 9102) at 1:1,000, CDK5 (Santa Cruz, sc-173) at 1:1,000, actin (Sigma-Aldrich, clone AC-74) at 1:10,000, c-Fos (Calbiochem, PC38) at 1:4,000, HA-HRP (Roche, clone 3F10) at 1:4,000, Myc-HRP (Santa Cruz, clone 9E10) at 1:3,000.

Mouse models

Preso1$^{-/-}$ mice were generated as follows. A 13-kb NheI BAC fragment containing exon 3 of *Preso1* was subcloned into the pBS vector. Exon 3 was released by Bsu36I and BstBI and subcloned into a loxP/PGK-neo vector. The *Preso1* targeting construct was generated by inserting the loxP/PGK-neo/Exon 3 back into Bsu36I and BstBI sites of the 13-kb BAC fragment of the mouse *Preso1* gene (Supplementary Fig. 7). The resulting targeting construct was linearized and electroporated into ES cells. ES cells were selected with G-418, and clones were picked, screened by PCR, and confirmed by Southern blotting for homologous recombination. Correctly targeted ES cell clones were injected into blastocysts, and chimeras were mated to C57BL/6 mice to produce *Preso1* floxed heterozygotes. These *Preso1* floxed heterozygotes were mated to *CMV-cre* mice to produce *Preso1*$^{+/-}$ mice, which were crossed to generate WT and *Preso1*$^{-/-}$ mice.

Grm5$^{-/-}$ (*mGluR5*$^{-/-}$) mice were obtained from John Roder[50]. *Grm5*$^{R/R}$ (mGluR5FR) mice replace the mGluR5 gene with a mutant that does not bind Homer, and were described previously[33]. *Homer2*$^{-/-}$*Homer3*$^{-/-}$ mice were generated as previously reported[22], and are healthy, fertile and not different from WT mice in size or behavior by casual observation.

Mice were group housed in plastic mouse cages with free access to standard rodent chow and water. The colony room was maintained at 22 ± 2 °C with a 12 h:12 h light:dark cycle. *Preso1*$^{-/-}$ mice were backcrossed at least five generations onto C57/Bl6J mice, and all the experiments were performed on littermate controls and blind to mouse genotype. *Grm5*$^{-/-}$ mice, *Grm5*$^{R/R}$ mice or *Homer2*$^{-/-}$*Homer3*$^{-/-}$ mice and their age-matched, same-background WT mice were used in all the experiments. Only adult male mice were used for behavioral experiments, and total 250 mice were used for all the experiments. All experiments were performed under protocols approved by the Animal Care and Use Committee of Johns Hopkins University School of Medicine for mice and rats.

Cell culture and transfection

HEK293T cells were cultured in DMEM medium with 10% FBS. Transfections were performed with Fugene 6 to manufacture's specifications. Cells were harvested 2 d after transfection.

Neuronal culture and electroporation

Neuronal cortical cultures from embryonic day 18 pups were prepared as reported previously[30]. Dorsal spinal cord neurons were prepared from embryonic day 15 pups. 5×10^5 neurons were added to each well of a 12-well plate (Corning) with cover slips coated

with poly-L-lysine. Growth medium consisted of MEM (Invitrogen) supplemented with 5% horse serum (Hyclone), 2% B27, 1% glutamine (Invitrogen), 100 U/ml penicillin, and 100 U/ml streptomycin (Invitrogen). Neurons were fed twice per week with glia-conditioned growth medium. DIV 14 neurons were used for calcium imaging. For the rescue experiment, electroporation was performed using a Nucleofector kit (Amaxa) after neuron dissociation. Calcium imaging was performed after 2 d.

Coimmunoprecipitation assays

Mouse brain tissues or HEK293T cells were used for the coimmunoprecipitation assay as previous reported[30]. Briefly, 500 microliters of immunoprecipitation buffer (PBS, pH 7.4, with 5 mM EDTA, 5 mM EGTA, 1 mM Na_3VO_4, 10 mM sodium pyrophosphate, 50 mM NaF, and 1% Triton X-100) containing Complete EDTA-Free protease inhibitors (Roche) was added and samples were sonicated. After centrifugation, the supernatant (300 μl) was then mixed with 0.5–2 μg of the appropriate antibody for 3 h at 4 °C. Then 50 μl of 1:1 protein A– or protein G–Sepharose slurry (Amersham-Pharmacia Biotech) was added for an additional 1 h. The protein beads were washed three times with immunoprecipitation buffer containing 1% Triton X-100. The protein samples were eluted with SDS loading buffer and analyzed by gel electrophoresis and western blotting.

Surface biotinylation assay

DIV 14 cortical neurons were used for surface biotinylation assay as previously reported[30]. Briefly, cortical neurons were cooled on ice, washed twice with ice-cold PBS++ (PBS, 1 mM $CaCl_2$, 0.5 mM $MgCl_2$) and then incubated with PBS++ containing 1 mg/ml sulfo-NHS-SS-biotin (Pierce) for 30 min at 4 °C. Unreacted biotin was quenched by washing cells three times with PBS++ containing 100 mM glycine (pH 7.4) (briefly once and for 5 min twice). Cultures were harvested in RIPA buffer and sonicated. Homogenates were centrifuged at 13,200 r.p.m. (16,100*g*) for 20 min at 4 °C. Fifteen percent of the supernatant was saved as the total protein. The remaining 85% of the homogenate was rotated with streptavidin beads (Pierce) for 2 h. Precipitates were washed with RIPA buffer three times (5 min each time). All procedures were done at 4 °C.

Immunoelectron microscopy

Immunoelectron microscopy was performed by postfixation immunogold labeling as described[51], using rabbit Preso1 antibody against the Preso1 C-terminal 20 aa.

Immunohistochemistry

Mouse spinal cord L4–5 sections were washed in PBS and incubated with 0.3% H_2O_2 in PBS for 30 min. After washing with PBS, sections were then blocked for 2 h at room temperature in blocking solution. c-Fos antibody was diluted in blocking solution (1:4,000) and incubated with sections overnight at 4 °C. After washing with PBS six times, sections were processed using an ABC kit (Vector) according to the manufacturer's instructions. Slices were mounted and photographed with a Nikon microscope.

Calcium imaging

HEK293T cells were loaded at 37 °C in aCSF buffer with 1 μM Fura-2/AM for 45 min. Dorsal spinal cord neurons were loaded at room temperature in aCSF buffer with 1 μM Fura-2/AM for 30 min. Ratiometric Ca^{2+} imaging was performed at 340 and 380 nm in 2 mM Ca^{2+} solution with a Nikon Eclipse 2000-U inverted microscope equipped with a fluorescence arc lamp, excitation filter wheel, and a Hamamatsu Orca CCD camera. Images were collected with Openlab (Improvision) and analyzed with Igor Pro.

Electrophysiology

Group I mGluR–coupled calcium current in the SCG neurons was measured as previously reported[7]. Briefly, both ganglia were removed from adult male Wistar rats (175–225 g, total 14 rats) following CO_2 euthanasia and decapitation, enzymatically and mechanically dissociated, and cultured overnight at 37 °C. Patch clamp experiments were performed the following day. All mGluR1 and mGluR5 constructs were injected at 100–130 ng μl^{-1} (pCDNA3.1+; Invitrogen); Preso1 was injected at 100 ng/μl where indicated. All neurons were coinjected with enhanced green fluorescent protein cDNA (0.02 μg / μl; pEGFPN1; BD Biosciences-Clontech, Palo Alto, CA) for identification of expressing cells.

Whole-cell current-clamp recordings were made using cultured DRG neurons. DRG neurons were cultured on cover slips for 1 d, and were transferred into a chamber with medium (the extracellular solution: ECS) of the following composition (in mM): NaCl 140, KCl 4, $CaCl_2$ 2, $MgCl_2$ 2, HEPES 10, glucose 5, with pH adjusted to 7.39 using NaOH and osmolarity adjusted to 310 mOsm with sucrose. The intracellular pipette solution (ICS) contained (in mM): KCl 135, Mg-ATP 3, Na_2-ATP 0.5, $CaCl_2$ 1.1, EGTA 2, HEPES 10, glucose 5, with pH adjusted to 7.36 using KOH and osmolarity adjusted to 300 mOsm with sucrose. In current clamp recordings, action potential measurements were performed with an Axon 700B amplifier and the pCLAMP 9.2 software package (Axon Instruments). All experiments were performed at room temperature (~25 °C).

Behavioral assays

Inflammatory pain responsiveness was assessed using formalin, as described[52]. Mice were injected subcutaneously with formalin (10 μl, 5% in saline) into the dorsal side of one hind paw. The total time spent licking or biting the injected hind paw was recorded during each 5-min interval for 60 min. For pharmacologic studies, MPEP (30 mg/kg in 10% Tween-80; Tocris) was administered subcutaneously 20 min before formalin injection.

CFA-induced pain response was performed as described[53]. Briefly, the intra-plantar region of one hind paw of each mouse was injected with 6 μl 50% CFA solution in saline. Thermal-pain sensitivity was assessed by recording paw withdrawal latency on exposure to a defined radiant-heat stimulus (Hargreaves test) before CFA injection and 1–5 d after injection.

Statistical analysis

All data were analyzed by two-tailed Student's *t*-test except the behavior data, which were analyzed by one-way ANOVA. Values are presented as means ± 95% confidence interval.

Supplementary Material

Refer to Web version on PubMed Central for supplementary material.

Acknowledgments

We thank J. Roder of University of Toronto for *Grm5*$^{-/-}$ mice, J. Worley for help with behavioral experiments and Y.-X. Wang for help with the immunogold. This work was supported by US National Institutes of Health grants from the National Institute on Drug Abuse (DA010309), National Institute of Mental Health (MH084020) and National Institute of Neurological Disorders and Stroke (NS050274 (P.F.W.); NS054791 and GM087369 (X.D.)); National 973 Basic Research Program of China (20009CB941400; B.X.); and the National Institute on Deafness and Other Communication Disorders Intramural Research Program (R.S.P.).

References

1. Lüscher C, Huber KM. Group 1 mGluR-dependent synaptic long-term depression: mechanisms and implications for circuitry and disease. Neuron. 2010; 65:445–459. [PubMed: 20188650]
2. Chiamulera C, et al. Reinforcing and locomotor stimulant effects of cocaine are absent in mGluR5 null mutant mice. Nat Neurosci. 2001; 4:873–874. [PubMed: 11528416]
3. Bhave G, Karim F, Carlton SM, Gereau RWt. Peripheral group I metabotropic glutamate receptors modulate nociception in mice. Nat Neurosci. 2001; 4:417–423. [PubMed: 11276233]
4. Niswender CM, Conn PJ. Metabotropic glutamate receptors: physiology, pharmacology, and disease. Annu Rev Pharmacol Toxicol. 2010; 50:295–322. [PubMed: 20055706]
5. Lujan R, Nusser Z, Roberts JD, Shigemoto R, Somogyi P. Perisynaptic location of metabotropic glutamate receptors mGluR1 and mGluR5 on dendrites and dendritic spines in the rat hippocampus. Eur J Neurosci. 1996; 8:1488–1500. [PubMed: 8758956]
6. Torres GE, Amara SG. Glutamate and monoamine transporters: new visions of form and function. Curr Opin Neurobiol. 2007; 17:304–312. [PubMed: 17509873]
7. Kammermeier PJ, Xiao B, Tu JC, Worley PF, Ikeda SR. Homer proteins regulate coupling of group I metabotropic glutamate receptors to N-type calcium and M-type potassium channels. J Neurosci. 2000; 20:7238–7245. [PubMed: 11007880]
8. Tu JC, et al. Homer binds a novel proline-rich motif and links group 1 metabotropic glutamate receptors with IP3 receptors. Neuron. 1998; 21:717–726. [PubMed: 9808459]
9. Park S, et al. Elongation factor 2 and fragile X mental retardation protein control the dynamic translation of Arc/Arg3.1 essential for mGluR-LTD. Neuron. 2008; 59:70–83. [PubMed: 18614030]
10. Wang JQ, Fibuch EE, Mao L. Regulation of mitogen-activated protein kinases by glutamate receptors. J Neurochem. 2007; 100:1–11. [PubMed: 17018022]
11. Hou L, Klann E. Activation of the phosphoinositide 3-kinase-Akt-mammalian target of rapamycin signaling pathway is required for metabotropic glutamate receptor-dependent long-term depression. J Neurosci. 2004; 24:6352–6361. [PubMed: 15254091]
12. Galante M, Diana MA. Group I metabotropic glutamate receptors inhibit GABA release at interneuron-Purkinje cell synapses through endocannabinoid production. J Neurosci. 2004; 24:4865–4874. [PubMed: 15152047]
13. Brakeman PR, et al. Homer: a protein that selectively binds metabotropic glutamate receptors. Nature. 1997; 386:284–288. [PubMed: 9069287]
14. Ango F, et al. Agonist-independent activation of metabotropic glutamate receptors by the intracellular protein Homer. Nature. 2001; 411:962–965. [PubMed: 11418862]
15. Dhavan R, Tsai LH. A decade of CDK5. Nat Rev Mol Cell Biol. 2001; 2:749–759. [PubMed: 11584302]
16. Lee HW, et al. Preso, a novel PSD-95-interacting FERM and PDZ domain protein that regulates dendritic spine morphogenesis. J Neurosci. 2008; 28:14546–14556. [PubMed: 19118189]
17. Zhong H, et al. Subcellular dynamics of type II PKA in neurons. Neuron. 2009; 62:363–374. [PubMed: 19447092]
18. An N, Blumer JB, Bernard ML, Lanier SM. The PDZ and band 4.1 containing protein Frmpd1 regulates the subcellular location of activator of G-protein signaling 3 and its interaction with G-proteins. J Biol Chem. 2008; 283:24718–24728. [PubMed: 18566450]
19. Xiao B, et al. Homer regulates the association of group 1 metabotropic glutamate receptors with multivalent complexes of homer-related, synaptic proteins. Neuron. 1998; 21:707–716. [PubMed: 9808458]
20. Hoover KB, Bryant PJ. The genetics of the protein 4.1 family: organizers of the membrane and cytoskeleton. Curr Opin Cell Biol. 2000; 12:229–234. [PubMed: 10712924]
21. Sharrocks AD, Yang SH, Galanis A. Docking domains and substrate-specificity determination for MAP kinases. Trends Biochem Sci. 2000; 25:448–453. [PubMed: 10973059]
22. Huang GN, et al. NFAT binding and regulation of T cell activation by the cytoplasmic scaffolding Homer proteins. Science. 2008; 319:476–481. [PubMed: 18218901]

23. Orlando LR, et al. Phosphorylation of the homer-binding domain of group I metabotropic glutamate receptors by cyclin-dependent kinase 5. J Neurochem. 2009; 110:557–569. [PubMed: 19457112]
24. Kammermeier PJ, Ikeda SR. Expression of RGS2 alters the coupling of metabotropic glutamate receptor 1a to M-type K+ and N-type Ca2+ channels. Neuron. 1999; 22:819–829. [PubMed: 10230801]
25. Gallagher SM, Daly CA, Bear MF, Huber KM. Extracellular signal-regulated protein kinase activation is required for metabotropic glutamate receptor-dependent long-term depression in hippocampal area CA1. J Neurosci. 2004; 24:4859–4864. [PubMed: 15152046]
26. Segal RA, Greenberg ME. Intracellular signaling pathways activated by neurotrophic factors. Annu Rev Neurosci. 1996; 19:463–489. [PubMed: 8833451]
27. Kitano J, et al. Tamalin, a PDZ domain-containing protein, links a protein complex formation of group 1 metabotropic glutamate receptors and the guanine nucleotide exchange factor cytohesins. J Neurosci. 2002; 22:1280–1289. [PubMed: 11850456]
28. Ferreira LT, et al. Calcineurin inhibitor protein (CAIN) attenuates Group I metabotropic glutamate receptor endocytosis and signaling. J Biol Chem. 2009; 284:28986–28994. [PubMed: 19717561]
29. Wang H, et al. Norbin is an endogenous regulator of metabotropic glutamate receptor 5 signaling. Science. 2009; 326:1554–1557. [PubMed: 20007903]
30. Hu JH, et al. Homeostatic scaling requires group I mGluR activation mediated by Homer1a. Neuron. 2010; 68:1128–1142. [PubMed: 21172614]
31. Hunskaar S, Hole K. The formalin test in mice: dissociation between inflammatory and non-inflammatory pain. Pain. 1987; 30:103–114. [PubMed: 3614974]
32. Puig S, Sorkin LS. Formalin-evoked activity in identified primary afferent fibers: systemic lidocaine suppresses phase-2 activity. Pain. 1996; 64:345–355. [PubMed: 8740613]
33. Cozzoli DK, et al. Binge drinking upregulates accumbens mGluR5-Homer2–PI3K signaling: functional implications for alcoholism. J Neurosci. 2009; 29:8655–8668. [PubMed: 19587272]
34. Sheng M, McFadden G, Greenberg ME. Membrane depolarization and calcium induce c-fos transcription via phosphorylation of transcription factor CREB. Neuron. 1990; 4:571–582. [PubMed: 2157471]
35. Alvarez FJ, Villalba RM, Carr PA, Grandes P, Somohano PM. Differential distribution of metabotropic glutamate receptors 1a, 1b, and 5 in the rat spinal cord. J Comp Neurol. 2000; 422:464–487. [PubMed: 10861520]
36. Kim SJ, et al. Transient upregulation of postsynaptic IP3-gated Ca release underlies short-term potentiation of metabotropic glutamate receptor 1 signaling in cerebellar Purkinje cells. J Neurosci. 2008; 28:4350–4355. [PubMed: 18434513]
37. Gainetdinov RR, Premont RT, Bohn LM, Lefkowitz RJ, Caron MG. Desensitization of G protein-coupled receptors and neuronal functions. Annu Rev Neurosci. 2004; 27:107–144. [PubMed: 15217328]
38. Dhami GK, Ferguson SS. Regulation of metabotropic glutamate receptor signaling, desensitization and endocytosis. Pharmacol Ther. 2006; 111:260–271. [PubMed: 16574233]
39. Bernier SG, Haldar S, Michel T. Bradykinin-regulated interactions of the mitogen-activated protein kinase pathway with the endothelial nitric-oxide synthase. J Biol Chem. 2000; 275:30707–30715. [PubMed: 10899167]
40. Hu HJ, Alter BJ, Carrasquillo Y, Qiu CS, Gereau RW. Metabotropic glutamate receptor 5 modulates nociceptive plasticity via extracellular signal-regulated kinase-Kv4.2 signaling in spinal cord dorsal horn neurons. J Neurosci. 2007; 27:13181–13191. [PubMed: 18045912]
41. Utreras E, Futatsugi A, Pareek TK, Kulkarni AB. Molecular Roles of Cdk5 in Pain Signaling. Drug Discov Today Ther Strateg. 2009; 6:105–111. [PubMed: 21253436]
42. Tronson NC, et al. Metabotropic glutamate receptor 5/Homer interactions underlie stress effects on fear. Biol Psychiatry. 2010; 68:1007–1015. [PubMed: 21075228]
43. Latremoliere A, Woolf CJ. Central sensitization: a generator of pain hypersensitivity by central neural plasticity. J Pain. 2009; 10:895–926. [PubMed: 19712899]

44. Neugebauer V, Li W, Bird GC, Bhave G, Gereau RWt. Synaptic plasticity in the amygdala in a model of arthritic pain: differential roles of metabotropic glutamate receptors 1 and 5. J Neurosci. 2003; 23:52–63. [PubMed: 12514201]
45. Bear MF. Therapeutic implications of the mGluR theory of fragile X mental retardation. Genes Brain Behav. 2005; 4:393–398. [PubMed: 16098137]
46. Rocher JP, et al. mGluR5 negative allosteric modulators overview: a medicinal chemistry approach towards a series of novel therapeutic agents. Curr Top Med Chem. 2011; 11:680–695. [PubMed: 21261592]
47. Yuan JP, et al. Homer binds TRPC family channels and is required for gating of TRPC1 by IP3 receptors. Cell. 2003; 114:777–789. [PubMed: 14505576]
48. Choi KY, Satterberg B, Lyons DM, Elion EA. Ste5 tethers multiple protein kinases in the MAP kinase cascade required for mating in *S. cerevisiae*. Cell. 1994; 78:499–512. [PubMed: 8062390]
49. Wong W, Scott JD. AKAP signalling complexes: focal points in space and time. Nat Rev Mol Cell Biol. 2004; 5:959–970. [PubMed: 15573134]
50. Lu YM, et al. Mice lacking metabotropic glutamate receptor 5 show impaired learning and reduced CA1 long-term potentiation (LTP) but normal CA3 LTP. J Neurosci. 1997; 17:5196–5205. [PubMed: 9185557]
51. Petralia RS, et al. Selective acquisition of AMPA receptors over postnatal development suggests a molecular basis for silent synapses. Nat Neurosci. 1999; 2:31–36. [PubMed: 10195177]
52. Kim AY, et al. Pirt, a phosphoinositide-binding protein, functions as a regulatory subunit of TRPV1. Cell. 2008; 133:475–485. [PubMed: 18455988]
53. Liu Q, et al. Sensory neuron-specific GPCR Mrgprs are itch receptors mediating chloroquine-induced pruritus. Cell. 2009; 139:1353–1365. [PubMed: 20004959]

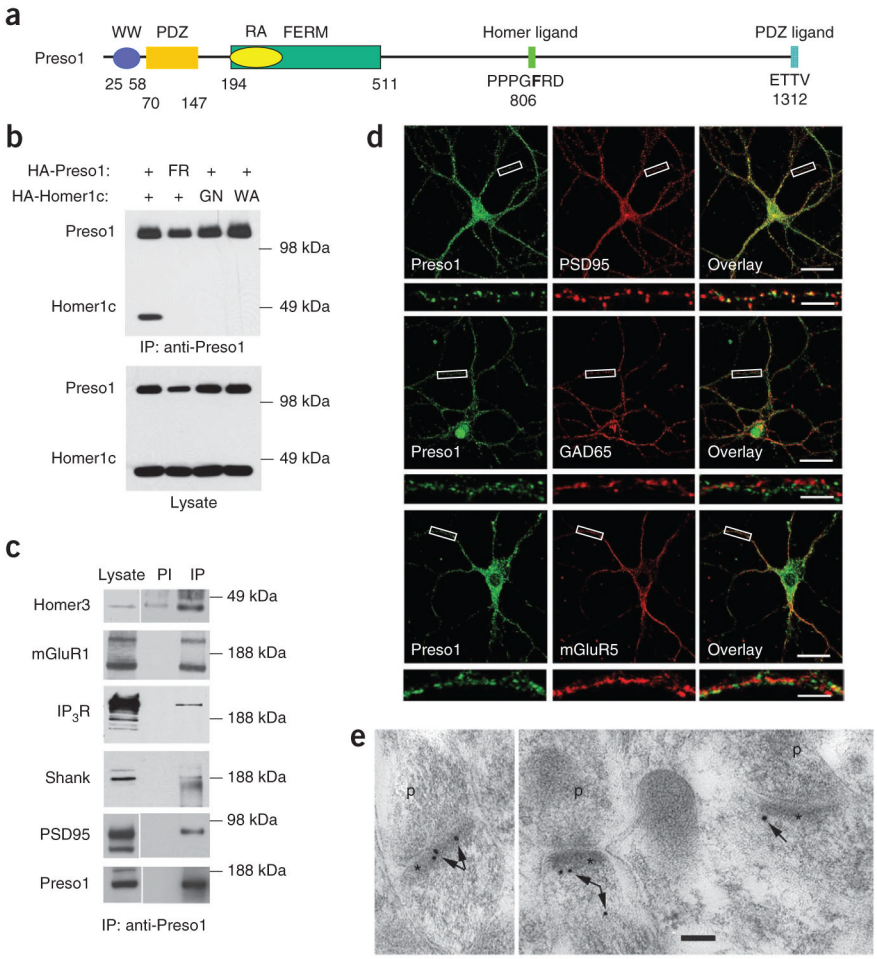

Figure 1.

Preso1 binds to Homer and localizes to the postsynaptic density. (**a**) Domain structure of rat Preso1 protein. F806, Homer binding site. (**b**) Various Preso1 and Homer constructs were transfected into HEK293T cells. Anti-Preso1 immunoprecipitated Homer1c, and this was disrupted by the F806R (FR) mutation in Preso1, or G89N (GN) or W24A (WA) mutation in Homer1c. (**c**) Rat cerebellum was lysed and incubated with anti-Preso1. Homer3, mGluR1, IP_3R, Shank and PSD95 immunoprecipitated with Preso1. PI, preimmune serum control; IP, immunoprecipitation. (**d**) Cultured hippocampal neurons immunostained with anti-Preso1 along with anti-PSD95 or anti-GAD65. Preso1 colocalized with PSD95 (a marker for excitatory synapses), but not with GAD65 (a marker for GABAergic inhibitory synapses). Scale bars represent 30 μm in main panels, 5 μm in the magnified dendrites (boxed). (**e**) Immunogold electron microscopy labeling of Preso1 in the hilus of the adult hippocampus. Gold particles (arrows) are enriched in and subjacent to the postsynaptic density (*). p, presynaptic terminal. Scale bar, 100 nm. Full-length western blots for this figure are shown in Supplementary Figure 9.

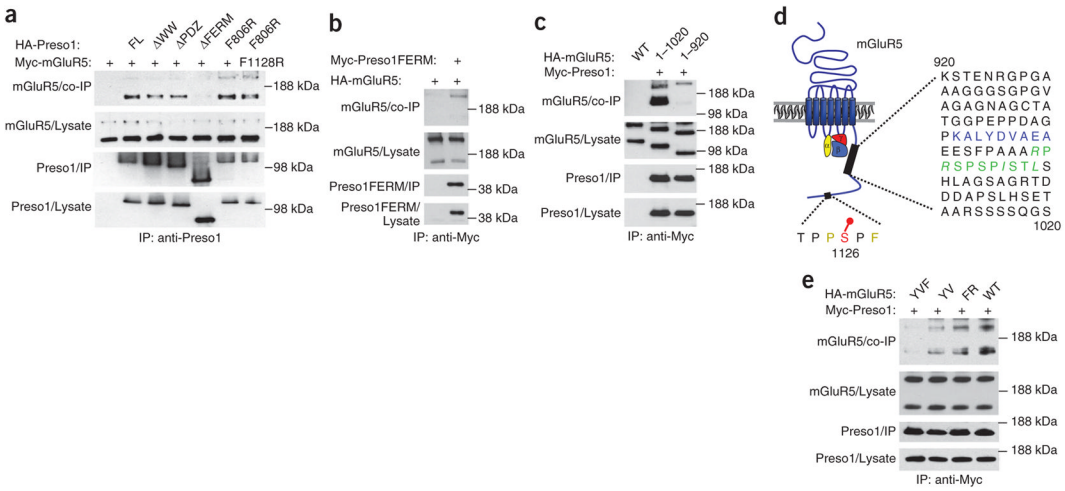

Figure 2.

Preso1 binds to the mGluR5 C terminus by means of its FERM domain. (**a**) mGluR5 and progressive N-terminal deletion and point mutants of Preso1 were cotransfected into HEK293T cells. Detergent lysates were incubated with anti-Preso1 and analyzed by western blotting with anti-HA. FL, Full length. ΔWW, ΔPDZ and ΔFERM delete the indicated domain from the N terminus. Only the Preso1-ΔFERM mutant failed to bind mGluR5. (**b**) The Preso1 FERM domain is sufficient to bind mGluR5. Preso1FERM and mGluR5 constructs were cotransfected into HEK293T cells, and detergent lysates were incubated with anti-Myc and analyzed by western blotting with anti-HA or anti-Myc. (**c**) Region of mGluR5 between amino acids 920 and 1020 is critical for its interaction with Preso1. Preso1 and various mGluR5 mutants were cotransfected into HEK293T cells. Detergent lysates were incubated with anti-Myc and analyzed by western blotting with anti-HA or anti-Myc. (**d**) mGluR5 structure showing the amino acid sequence between 920 and 1020 and Homer ligand. A predicted binding site for Preso1 FERM domain is shown in blue; a predicted D-domain for ERK binding is shown in green, with critical amino acids italicized. The Homer binding site is shown in yellow, and phosphorylation site in red. (**e**) Preso1 and various mGluR5 mutants were cotransfected into HEK293T cells and assayed for coimmunoprecipitation. Mutation of mGluR5 FERM (Y965A, V967A; YV) and mGluR5 Homer (F1128R; FR) binding sites (mGluR5 YVF) abolished Preso1 binding. Full-length western blots for this figure are shown in Supplementary Figure 10.

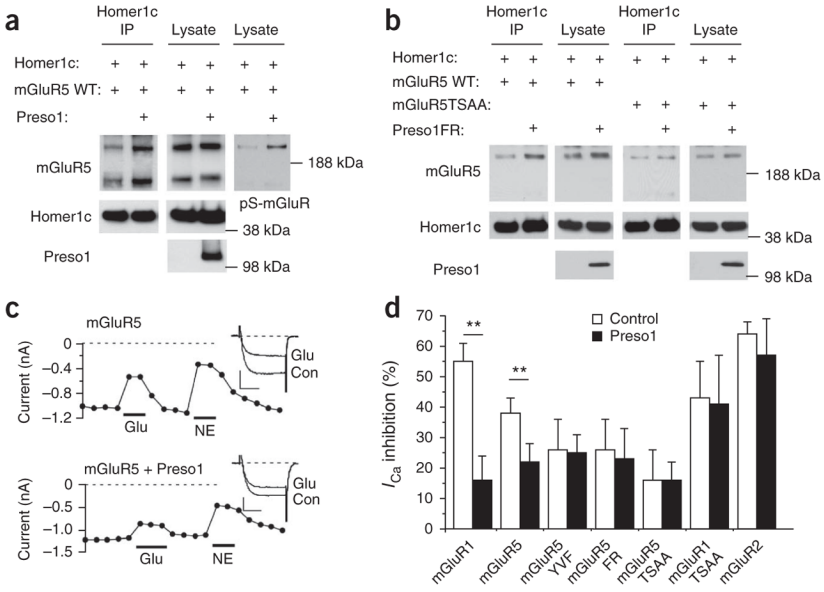

Figure 3.

Preso1 enhances mGluR5 phosphorylation and Homer–mGluR5 binding, and inhibits group I mGluR coupling to voltage-gated Ca^{2+} channels. (**a**) HA-tagged Homer1c, HA-tagged mGluR5 and HA-tagged Preso1 constructs were cotransfected into HEK293T cells. Lysates were immunoprecipitated with anti-Homer1c and analyzed by western blotting with anti-HA. Lysates were also blotted with anti–pSer-mGluR (right). (**b**) Preso1-dependent enhancement of mGluR5–Homer binding requires phosphorylation sites of mGluR5, but does not require Homer binding to Preso1. HA-tagged Homer1c, HA-tagged mGluR5TSAA and HA-tagged Preso1FR constructs were cotransfected into HEK293T cells. Same analysis as **a**. $n = 6$ for each group. (**c**,**d**) Coupling of group I mGluRs to voltage-gated calcium channels in superior cervical ganglion neurons. (**c**) Sample currents (inset) and time course illustrating reduction of inhibition by 100 μM glutamate but not 10 μM norepinephrine (NE) in a superior cervical ganglion neuron expressing mGluR5 with or without Preso1. Con, control; Glu, glutamate. (**d**) Expression of Preso1 reduces mGluR1/5-dependent modulation of calcium current by glutamate, and requires Homer binding and phosphorylation sites of mGluR1/5. Summary of data from cells expressing various mGluR constructs with or without Preso1: mGluR5YVF (does not bind Homer or Preso1), mGluR5FR (does not bind Homer), mGluR1/5TSAA (binds Homer but cannot be phosphorylated at the Homer binding site). Preso1 did not alter response of mGluR2. $n = 15, 11, 24, 22, 7, 8, 7, 11, 9, 13, 14, 6, 7, 5$, from left to right; $^{**}P < 0.01$. Error bars, 95% confidence intervals. Full-length western blots for this figure are shown in Supplementary Figure 11.

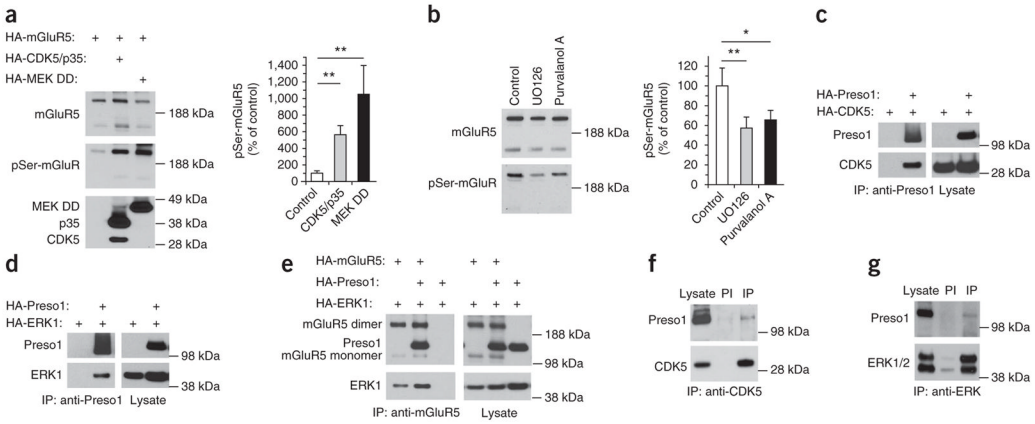

Figure 4.

Preso1 binds proline-directed kinases and enhances kinase-mGluR5 binding. (**a**) CDK5/p35 or MEK DD expression increases mGluR5 phosphorylation. HA-tagged mGluR5 and HA-CDK5/HA-p35 or HA-MEK DD (constitutively active) were cotransfected into HEK293T cells. Lysates were blotted with anti-mGluR5, anti–pSer-mGluR and anti-HA. Quantitation (below): $^{**}P < 0.01$, $n = 3$ each group. (**b**) Inhibitors of MEK (UO126, 4 μM) or CDK5 (purvalanol A, 20 μM) for 30 min reduced basal phosphorylation of mGluR5 in cortical neurons at 14 days *in vitro* (DIV). mGluR5 was immunoprecipitated and blotted with mGluR5 or pSer-mGluR. Quantitation (**a**,**b**, below): $^{*}P < 0.05$, $^{**}P < 0.01$, $n = 4$ for each group. (**c**) CDK5 immunoprecipitates with Preso1 from HEK293T cells. (**d**) ERK1 immunoprecipitates with Preso1 from HEK293T cells. (**e**) Preso1 increases immunoprecipitation of ERK1 with mGluR5. HA-tagged mGluR5 and HA-tagged Preso1 were cotransfected into HEK293T cells, and lysates were precipitated with anti-mGluR5 and blotted with anti-HA and anti-ERK1. (**f**) Preso1 immunoprecipitates with CDK5 from mouse brain detergent lysate. (**g**) Preso1 immunoprecipitates with ERK1/2 from mouse brain detergent lysate. PI, preimmune; IP, immunoprecipitation. Error bars, 95% confidence intervals. Full-length western blots for this figure are shown in Supplementary Figure 12.

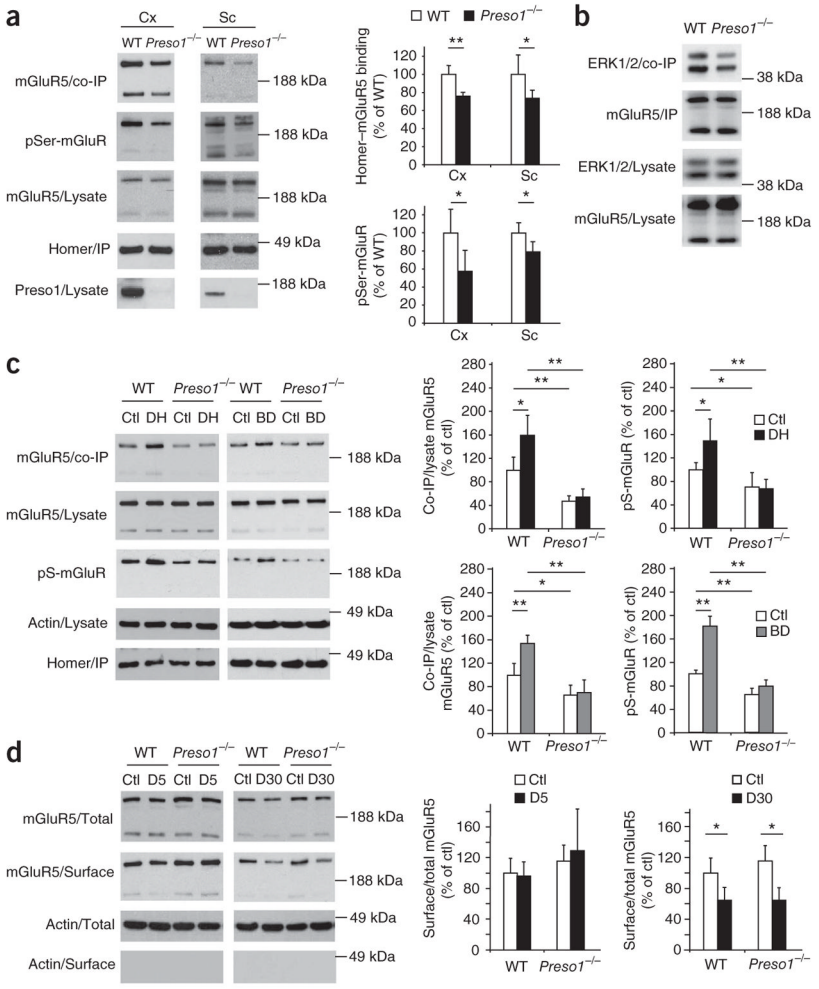

Figure 5.

Preso1 is required for activity-dependent increase of mGluR5 phosphorylation and Homer binding. (**a**) mGluR phosphorylation and Homer–mGluR5 coimmunoprecipitation are decreased in cortex and spinal cord of *Preso1*$^{-/-}$ mice. Cortex (Cx) and spinal cord (Sc) lysates from WT and *Preso1*$^{-/-}$ mice were blotted with anti–pSer-mGluR or immunoprecipitated with pan-anti-Homer and blotted with indicated antibodies. *$P < 0.05$, **$P < 0.01$, $n = 5$–8 for each group. (**b**) ERK1/2 immunoprecipitation with mGluR5 is decreased in *Preso1*$^{-/-}$mice. Forebrain lysates from WT and *Preso1*$^{-/-}$mice were immunoprecipitated with anti-mGluR5, and the lysates (bottom panels) and immunoprecipitates were blotted with anti-ERK or anti-mGluR5. (**c**) Activation of mGluR5 or BDNF receptor TrkB increases mGluR5 serine phosphorylation and Homer–mGluR5 coimmunoprecipitation in WT but not *Preso1*$^{-/-}$ DIV 14 cortical neurons. Cultures were treated with DHPG (DH; 100 μM) or BDNF (BD; 20 ng ml^{-1}) for 30 min and lysed for pan-Homer immunoprecipitation and western blot. Ctl, control. Quantitation (right): *$P < 0.05$, **$P < 0.01$, $n = 3$–8 for each group. (**d**) Surface and total expression of mGluR5 is not different between WT and *Preso1*$^{-/-}$ DIV 14 cortical neurons. Cultures were treated with DHPG (100 μM) for 5 min or 30 min and processed for surface biotinylation and western blotting. Quantitation (right): *$P < 0.05$, $n = 3$–6 for each group. D5, DHPG 5 min; D30, DHPG 30 min. Error bars, 95% confidence intervals. Full-length western blots for this figure are shown in Supplementary Figure 13.

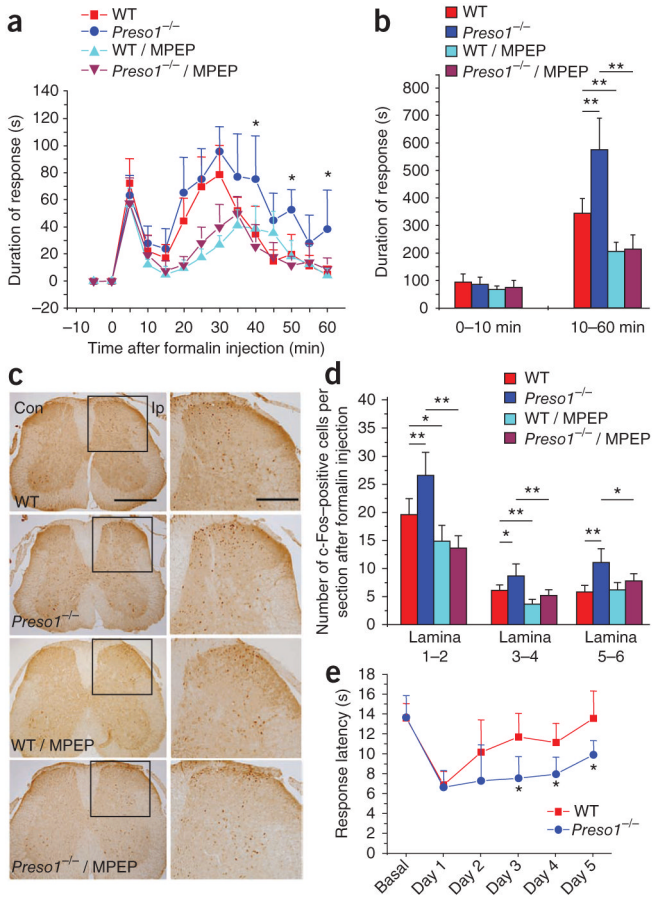

Figure 6.

Increased pain response to formalin or complete Freund's adjuvant in *Preso1*$^{-/-}$ mice. (**a**,**b**) Formalin-induced inflammatory pain is increased in *Preso1*$^{-/-}$ mice and is dependent on mGluR5. (**a**) The duration of behavioral responses to hind paw formalin injection in 5-min intervals comparing littermate WT and *Preso1*$^{-/-}$ mice with or without MPEP before injection. (**b**) Results from **a** grouped into two phases. *$P < 0.05$, **$P < 0.01$, $n = 6–9$ for each group. (**c**,**d**) Formalin-induced c-Fos expression in *Preso1*$^{-/-}$ mice. (**c**) c-Fos immunohistochemistry of L4–L5 of spinal cord 90 min after formalin. Boxed regions are magnified at right. Scale bars, 500 μm at left, 200 μm at right. Con, contralateral; Ip, ipsilateral. (**d**) Statistical data from **c**. $n = 18–25$ sections from 3–5 mice in each group. *$P < 0.05$, **$P < 0.01$. (**e**) Pain response to complete Freund's adjuvant is increased in *Preso1*$^{-/-}$ mice. Latency to withdrawal was monitored before and for 5 d after injection of complete Freund's adjuvant into hind paw of littermate WT and *Preso1*$^{-/-}$ mice. *$P < 0.05$, $n = 9$ for each group. Error bars, 95% confidence intervals.

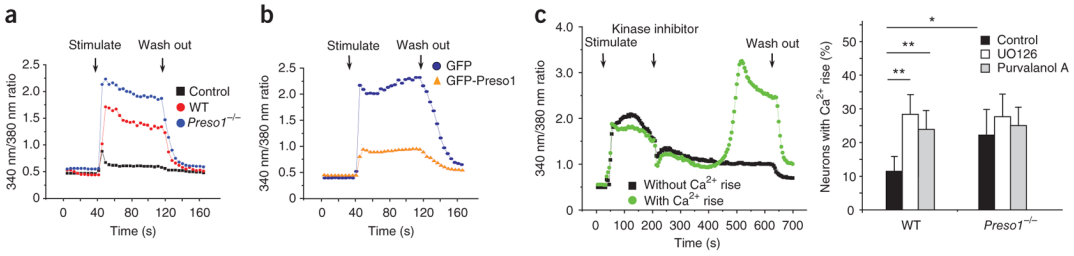

Figure 7.

Enhanced group I mGluR-mediated calcium response in the spinal cord neurons of *Preso1*$^{-/-}$ mice. (**a**) Representative traces (left) and population (right) peak Ca^{2+} responses of WT and *Preso1*$^{-/-}$ DIV 14 dorsal spinal cord neurons stimulated with glutamate (100 μM), APV (100 μM) and NBQX (100 μM). Pretreatment with group I mGluR antagonists Bay 36-7620 (mGluR1 antagonist, 20 μM) and MPEP (mGluR5 antagonist, 10 μM) blocked the Ca^{2+} response. Calcium concentration was measured by Fura-2 340 nm/380 nm ratio. n = 90 for WT neurons; n = 74 for *Preso1*$^{-/-}$ neurons. (**b**) A *Preso1* transgene reduces Ca^{2+} response in DIV 2 *Preso1*$^{-/-}$ dorsal spinal cord neurons. Representative traces and population responses of *Preso1*$^{-/-}$ neurons expressing GFP or GFP-Preso1. Same assay as in **a**; n = 23 for GFP neurons, n = 19 for GFP-Preso1 neurons. (**c**) MEK or CDK5 inhibitors increase the percentage of neurons showing a delayed Ca^{2+} increase in WT but not *Preso1*$^{-/-}$ dorsal spinal cord neurons. Neurons were stimulated as in **a**, and after 2 min, kinase inhibitors UO126 (4 μM) or purvalanol A (5 μM) or vehicle (control) were added, followed by washout at 10 min. Left panel shows traces of Ca^{2+} responses from WT neurons, with example of delayed rise of [Ca^{2+}] that reverses on washout. For WT neurons, n = 390 neurons in 8 experiments, 420 neurons in 9 experiments and 330 neurons in 10 experiments for vehicle, UO126 and purvalanol A, respectively. For *Preso1*$^{-/-}$ neurons, n = 360 neurons in 8 experiments, 270 neurons in 7 experiments and 190 neurons in 6 experiments for vehicle, UO126 and purvalanol A conditions, respectively. *P < 0.05, **P < 0.01. Error bars, 95% confidence intervals.